NOVEL NONLINEAR SPRING DESIGN FOR WIDEBAND VIBRATION ENERGY HARVESTERS

M. Amri[1,3*], P. Basset[1], F. Cottone[1], D. Galayko[2], F. Najar[3] and T. Bourouina[1]
[1]Université Paris-Est, ESYCOM, ESIEE Paris, Noisy-le-Grand, France
[2] LIP6, UPMC Universités Paris Sorbonne, Paris, France
[3]Université de Carthage, LASMAP, Ecole Polytechnique de Tunisie, La Marsa, Tunisie
*Presenting Author: m.amri@esiee.fr

Abstract: This paper presents the design and analysis of a novel nonlinear spring for widening the bandwidth of the frequency-response of a vibration energy harvester (VEH). Based on a crab-leg design, an angle α is introduced in the main spring beam in order to add geometric nonlinearities. We use a discrete optimization process to determine the optimal shape of the spring given by α. We present the correspondent frequency-response curves under ideal white-noise excitations using Lindstedt-Poincaré Perturbation Technique. It appears that the angle α maximizing nonlinearities is 170°. Based on this design, a VEH having two linear and two nonlinear springs is proposed for lowering the excitation frequency range.

Keywords: wideband vibration energy harvester, nonlinear oscillators, Lindstedt-Poincaré Perturbation Technique

INTRODUCTION

VEHs are currently receiving a great attention thanks to their ability to act as independent autonomous power generators for MEMS components. An efficient VEH has to operate in the mode of strong electromechanical coupling [1] and has to benefit to most of the vibration frequencies available in the surrounding environment. However most of those devices are designed as linear resonant structures. One of their fundamental limitations is their narrow bandwidths. A solution to overcome this problem is to introduce nonlinear springs, which introduces a hysterical mechanical behavior and their design can be complex [2].

In this work, we detail the optimization process used to determine the optimal shape of a novel nonlinear spring design, and we present an approach for the determination of the frequency response based on the Lindstedt-Poincaré Perturbation Technique. Then we modify the formula of the maximal harvested power for linear VEH [3] in order to evaluate the efficiency of the spring design.

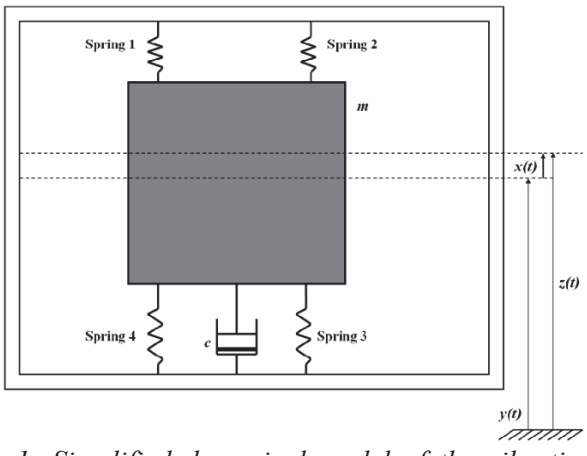

Fig. 1: Simplified dynamical model of the vibration-driven energy harvester.

DYNAMICAL MODEL

Model and equation of motion

We used a simplified spring-mass dynamical model of the vibration-driven energy harvester made of 4 springs, a damper and an inertial mass which dimensions and design rules are based on the silicon-based VEH in [4]. We assume that the oscillator is a single degree of freedom lumped system (Fig. 1). We denote by x its displacement in the mobile rigid frame and y the displacement of the frame itself. The governing equation of motion can be derived using Newton's second law as:

$$m\ddot{x} - F_d - F_R = F = -m\ddot{y} \quad (1)$$

where m is the effective mass of the resonator, $\ddot{x}$ and $\ddot{y}$ are the second time derivative of x and y, respectively. F_d is the damping force, F_R is the springs restoring force and F is the external force applied on the inertial mass by the rigid frame. We assume linear viscous damping that is:

$$F_d = -c\dot{x} \quad (2)$$

where c is the damping coefficient.

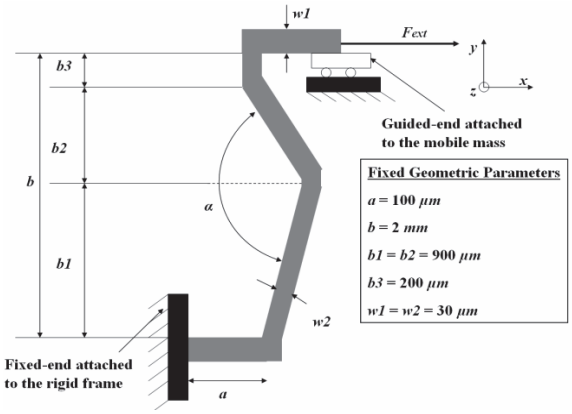

Fig. 2: Schematic view of the nonlinear spring.

Restoring force

First, we perform finite element analysis to derive the expression of F_R for the proposed spring in Fig. 2.

This geometry is based on a crab-leg design. An angle α is introduced in the main beam to add geometric nonlinearities [5] due to larger deformations, while keeping a low operational frequency range as we will see later.

For this design, the restoring force F_R is not proportional to x when oscillations amplitude is not negligible comparing to the spring thickness. We assume third order Taylor series expansion of the nonlinear restoring force, which is:

$$F_R = -(kx + k_1x^2 + k_2x^3) \quad (3)$$

where k is the normal linear spring constant, k_1 and k_2 are the second and third order corrections, respectively. Those constants depend on spring dimensions, geometric parameter α and boundary conditions. In all following analysis, the only variable parameter is the angle α that determines the shape of the spring. The fixed geometric parameters are mentioned in Fig. 2.

Using commercial FEM tool *ANSYS Multiphysics*, we apply a horizontal displacement on the guided end gradually and we determine the value of restoring force for each load increment. We plot the force-displacement curve in Fig. 3 for a set of angles. They are asymmetric due to the asymmetry of the spring geometry. For large displacements the curves are no more linear.

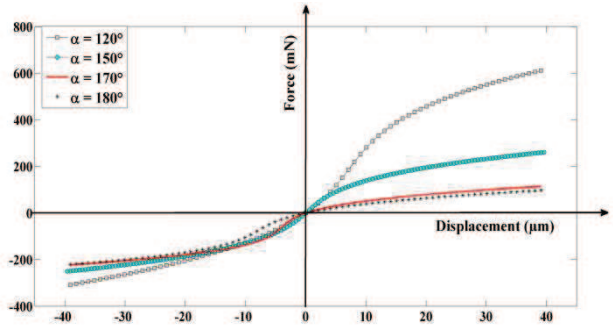

Fig. 3: Force-displacement curve of one nonlinear spring obtained by FEM for various values of α. 40 linear elements were used to model each spring segment.

We numerically evaluate the spring constants using the following optimization formulation based on least square method:

$$\min_{k,k_1,k_2} \left(\sum_{i=1}^{m} (F_{Ri} - (kx_i + k_1x_i^3 + k_2x_i^3)\right)^2 \quad (4)$$

where x_i is the displacement increment and F_{Ri} is the restoring force at the increment i. The obtained results are shown in Fig. 4 after fitting. k, k_1 and k_2 are maximal at $\alpha = 180°$. One may think that it is the best angle for nonlinearities. However, this is not exact as we will see later. In addition, the angle 180° leads to the stiffest springs resulting in the highest working frequency range comparing to other values of α. Indeed, the linear resonance frequency $\omega_0 = \sqrt{\frac{k}{m}}$ increases with k and is maximal at $\alpha = 180°$.

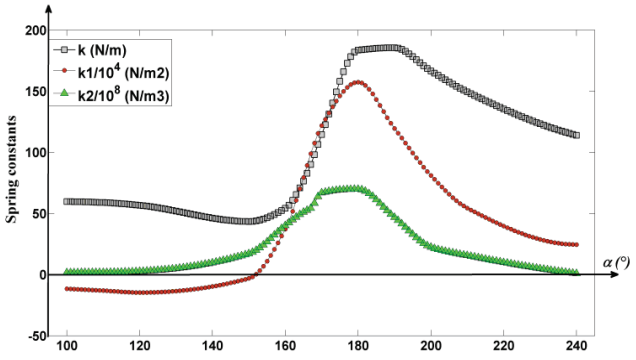

Fig. 4: Spring constants obtained by FEM, 40 linear elements were used to model each beam segment.

FREQUENCY-RESPONSE CURVES

We present results obtained by the Lindstedt-Poincaré Perturbation Technique [6-7] to determine the frequency-response curves of the oscillator. We also performed numerical solutions given by Long Time Integration method to validate the perturbation approach (not shown in this paper).

Lindstedt-Poincaré Perturbation Technique

Substituting F_R and F_d by their expressions in Eq. l) leads to:

$$m\ddot{x} + c\dot{x} + kx + k_1x^2 + k_2x^3 = F \quad (5)$$

We assume that the solution of Eq. 5) is periodic. Far from resonance, the nonlinear terms are small. The time harmonic vibration amplitude X can be written as [7]:

$$X = \frac{\frac{F_\omega}{m}}{\sqrt{(\omega^2 - \omega_0^2)^2 + (\frac{\omega\omega_0}{Q})^2}} \quad (6)$$

where F_ω is the magnitude of the forcing term at frequency ω and $Q = \frac{\omega_0 m}{c}$ denotes the quality factor.

Near resonance, frequency-response curves can be approximated using the Lindstedt-Poincaré Perturbation Technique. We first consider unforced-undamped vibrations:

$$m\ddot{x} + kx + k_1x^2 + k_2x^3 = 0 \quad (7)$$

We introduce the perturbation parameter ε. We assume that the nonlinear terms in Eq. 7) will change the resonance frequency to ω_0'. Then x and ω_0' can be written as:

$$\begin{cases} x = x_0 + \varepsilon x_1 + \varepsilon^2 x_2 \\ \omega_0' = \omega_0 + \varepsilon\omega_1 + \varepsilon^2\omega_2 \end{cases} \quad (8)$$

Solving Eq. 7) and Eq. 8) for oscillations amplitude X_0 leads to [7]:

$$X_0 = \frac{\frac{F_\omega}{m}}{\sqrt{(\omega^2 - \omega_0'^2)^2 + (\frac{\omega\omega_0'}{Q})^2}} \quad (9)$$

where $\omega_0' = \omega_0 + \kappa X_0^2$ is the new resonance frequency that depends on oscillations amplitude and κ denotes the nonlinear spring constant that measures the change of the resonance frequency. κ is defined as [7]:

$$\kappa = \frac{3k_2}{8k}\omega_0 - \frac{3k_1^2}{12k^2}\omega_0 \quad (10)$$

From Fig. 5 it can be seen that the angle α leading to the best nonlinearity is 170°.

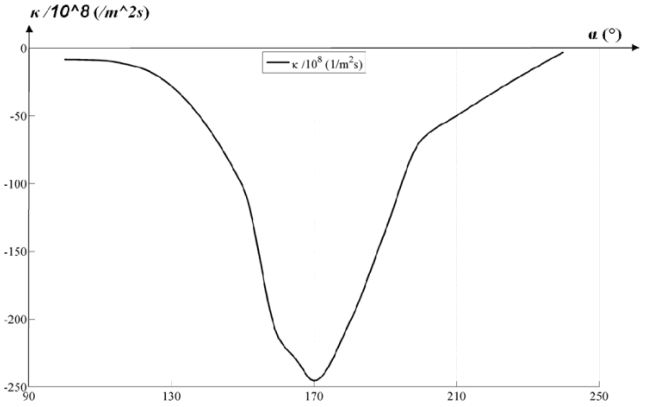

Fig. 5: Nonlinear effect constant κ versus the angle α for one nonlinear spring.

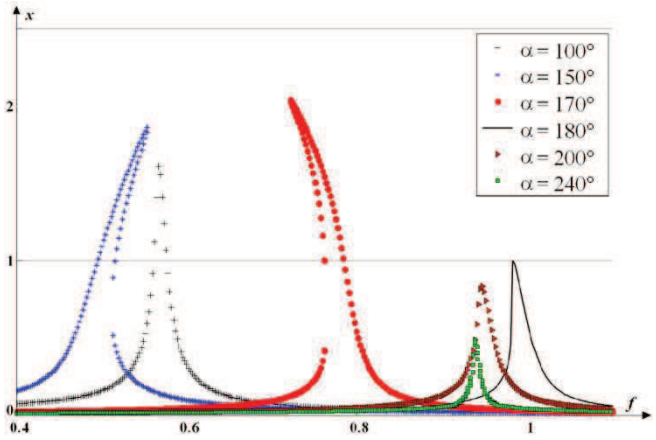

Fig. 6: Normalized amplitude versus normalized frequency of the mobile mass under harmonic excitations for various values of α (normalization is with respect to the values of α = 180°).

Fig. 6 shows that the angle α =180° leads to the higher working frequency range as expected. In addition, one can notice that when $\kappa' < 0$, a hardening effect is obtained and when $\kappa' \geq 0$, a softening effect is observed, where κ' is the first derivative of κ with respect to α.

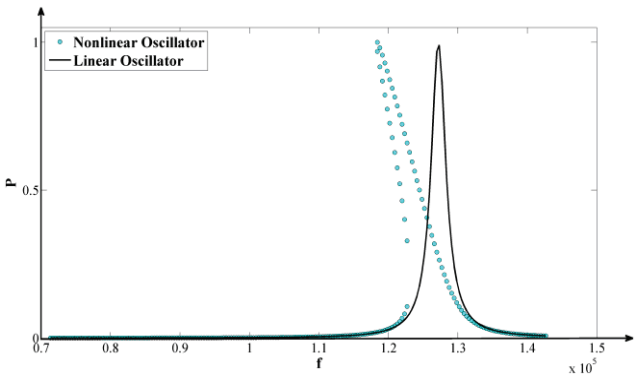

Fig. 8: Normalized power versus normalized frequency under harmonic excitations 0.5 g in amplitude. The reference angle is α =170°.

Convertible Power

If we assume that the mechanism responsible for the conversion of power from the mechanical domain to the electrical domain is equivalent to an ideal damper, the convertible energy is equivalent to the dissipated energy. For a linear oscillator the convertible power is equal to [3]:

$$P = \frac{\xi\omega_c^3 \omega m Y_0^2 \omega^3}{(1-\omega_c^2)^2 + (2\xi\omega_c)^2} \quad (11)$$

where $\omega_c = \frac{\omega}{\omega_0}$, $\xi = \frac{1}{2Q}$ is the damping ratio and Y_0 is the rigid frame displacement amplitude. Eq. 11) can be written as:

$$P = \frac{1}{2} c\omega^2 X_0^2 \quad (12)$$

To calculate the maximal convertible power of our structure near resonance, we substitute the linear resonant pulsation ω_0 by $\omega_0' = \omega_0 + \kappa X_0^2$ in Eq. 12).

Fig. 8 compares the frequency response of a linear and a nonlinear oscillator having the same linear spring stiffness, mass and damper. It can be seen that the two systems have almost the same peak amplitude. In order to evaluate the efficiency of each system, we calculate the average convertible power as:

$$\overline{P} = \frac{1}{n}\sum_{\varpi} P_\omega \quad (13)$$

where P_ω is the convertible power at the frequency ω and n denotes the number of frequencies. The average power generated by the nonlinear system is 2.6 times greater than the linear oscillator because it has a larger bandwidth.

We use the same method to calculate the average convertible power for different values of α when the system is subjected to a perfect white noise of different levels [8]. Fig. 9 shows that for small excitations, the behavior of the system is linear and the average convertible power is almost constant for all values of α (Fig. 9). Increasing the excitations amplitude leads to a nonlinear behavior. A peak power generation is observed at $\alpha = 170°$.

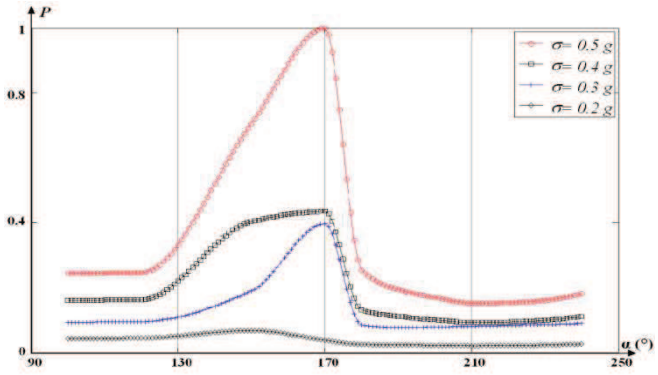

Fig. 9: Normalized output power versus α when the mobile mass is under ideal white noise excitation of standard deviation σ.

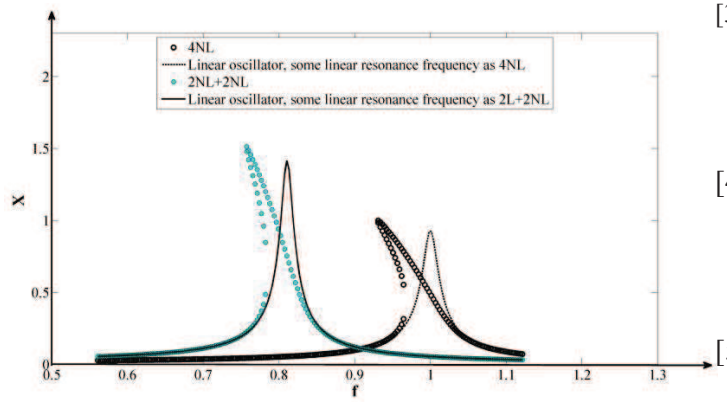

Fig. 10: Normalized amplitude versus normalized frequency when the mobile mass under ideal white noise excitation of standard deviation σ = 0.5 g.

Lowering the frequency range

In order to reach a lower working frequency range of the device, we propose to attach the inertial mass with 2 serpentine-shaped linear springs and two nonlinear springs. Fig. 10 shows the impact of such configuration.

It can be seen that the -3dB bandwidth of the design with a mix of linear and nonlinear springs is 125% larger than the fully linear configuration and could harvest 2.5 times more energy if excited by an ideal white noise. The device having 4 nonlinear springs has a -3dB bandwidth 147% larger than a linear oscillator with the same stiffness and could harvest 2.6 times more energy. In addition, we can see that the oscillation amplitude increases thanks to the proposed configuration.

CONCLUSION

Based on Lindstedt-Poincaré Perturbation Technique, a discrete optimization process is achieved to determine the optimal angle that maximizes the oscillations bandwidth. The angle does not only add nonlinearities to the motion of the system, but can also decrease the stiffness of the springs leading to lower operational frequency range. A VEH design having two linear springs and two nonlinear springs is proposed in order to reduce the operational frequency range.

REFERENCES

[1] Galayko D and Basset P 2011 A general analytical tool for the design of Vibration Energy Harvesters (VEH) based on the mechanical impedance concept – application to electrostatic transducers *IEEE Transactions on Circuits and Systems I: Regular Papers*, vol. **58**, n°2, 299-311

[2] Zhu D, Michael J T, Stephen P B 2010 Strategies For Increasing The Operating Frequency Range Of Vibration Energy Harvesters: A Review *Meas. Scien. and Tech.* **21** (2). 022001

[3] Mitcheson P D, Green T C,Yeatman E M, HolmesA S 2004 Architectures for Vibration-Driven Micropower Generators *IEEE J. Microelectromech. Syst.*, vol**. 13** , n°3, 429-439

[4] Basset P, Galayko D, Paracha A M, Marty F, Dudka A, Bourouina T 2009 A Batch-Fabricated and Electret-free Silicon Electrostatic Vibration Energy Harvester *J. Micromech. Microeng.,* **19** 115025

[5] Nguyen D S, Halvorsen E, Jensen G U, Vogl A 2010Fabrication and Characterization of a Wideband MEMS Energy Harvester Utilizing Nonlinear Springs *J. Micromech. Microeng* **20** 125009

[6] Nayfeh A H 1993 Introduction to Perturbation Techniques (USA, Wiley Classics Library Edition Published 1993) 159-176

[7] Kaajakari V, Mattila T, Oja A, Seppä H 2004 Nonlinear limits for single-crystal silicon Microresonators *IEEE J. Microelectromech. Syst* vol. **13**, n°5, 715-724

[8] Cottone F, Vocca H, Gammaitoni L 2009 Nonlinear energy harvesting *Phys. Rev. Lett.* **102** 080601